

Using inositol as a biocompatible ligand for efficient transgene expression

Lei Zhang¹
Susan L Bellis²
Yiwen Fan³
Yunkun Wu¹

¹State Key Laboratory of Structural Chemistry, Fujian Institute of Research on the Structure of Matter, Chinese Academy of Sciences, Fuzhou, People's Republic of China;

²Cell, Developmental and Integrative Biology, University of Alabama at Birmingham, Birmingham, AL, USA;

³Key Laboratory of Biomedical Polymers of Ministry of Education, Department of Chemistry, Wuhan University, Wuhan, People's Republic of China

Abstract: Transgene transfection techniques using cationic polymers such as polyethylenimines (PEIs) and PEI derivatives as gene vectors have shown efficacy, although they also have shortcomings. PEIs have decent DNA-binding capability and good cell internalization performance, but they cannot deliver gene payloads very efficiently to cell nuclei. In this study, three hyperbranched polyglycerol-polyethylenimine (PG6-PEI) polymers conjugated with myo-inositol (INO) molecules were developed. The three resulting PG6-PEI-INO polymers have an increased number of INO ligands per molecule. PG6-PEI-INO 1 had only 14 carboxymethyl INO (CMINO) units per molecule. PG6-PEI-INO 2 had approximately 130 CMINO units per molecule. PG6-PEI-INO 3 had as high as 415 CMINO units approximately. Mixing PG6-PEI-INO polymers with DNA produced compact nanocomposites. We then performed localization studies using fluorescent microscopy. As the number of conjugated inositol ligands increased in PG6-PEI-INO polymers, there was a corresponding increase in accumulation of the polymers within 293T cell nuclei. Transfection performed with spherical 293T cells yielded 82% of EGFP-positive cells when using PG6-PEI-INO 3 as the vehicle. Studies further revealed that extracellular adenosine triphosphate (eATP) can inhibit the transgene efficiency of PG6-PEI-INO polymers, as compared with PEI and PG6-PEI that were not conjugated with inositol. Our work unveiled the possibility of using inositol as an effective ligand for transgene expression.

Keywords: myo-inositol, nuclear localization, biocompatibility, polyglycerol-polyethylenimine, hyperbranched polymers, extracellular ATP

Introduction

Gene transfection techniques have been widely used in functional genomics and gene therapy research.^{1,2} Virus-derived vectors are known for their high gene delivery efficiency; however, these vectors also pose potential risks.³⁻⁵ Owing to the convenience in preparation and tailoring design, nonviral vectors based on natural or synthetic biomaterials have become highlighted.^{2,6-11}

Various barriers, including the nuclear membrane as the main barrier, exist before efficient transgene expression is achieved (Figure 1). Versatile gene carriers, including a class of intensively studied cationic polymers, such as branched polyethylenimine (PEI), poly-*N*-(2-hydroxypropyl) methacrylamide (poly-HPMA), poly(amido amine) dendrimers and chitosan, have been developed for transport of large nucleic acid payloads.²⁻⁸ These polymers can compact the nucleotides and help them escape from endosomal degradation through a "proton-sponge effect".^{6,12} Gene vectors with reduced cytotoxicity and immune recognition can be achieved through various modifications, for example, with poly-HPMA, polycaprolactone (PCL), and polyethylene glycol (PEG).¹³⁻¹⁷ Target approaches can enhance cell internalization of the gene delivery systems,¹⁸⁻²¹ but the cell-membrane-targeted ligands are not ideal

Correspondence: Yunkun Wu/Lei Zhang
State Key Laboratory of Structural Chemistry, Fujian Institute of Research on the Structure of Matter, Chinese Academy of Sciences, 155 Yangqiao Road West, Fuzhou 350002, People's Republic of China
Tel +86 591 8370 5554
Fax +86 591 8370 5554
Email ykwu@fjirsm.ac.cn; zhangl@fjirsm.ac.cn

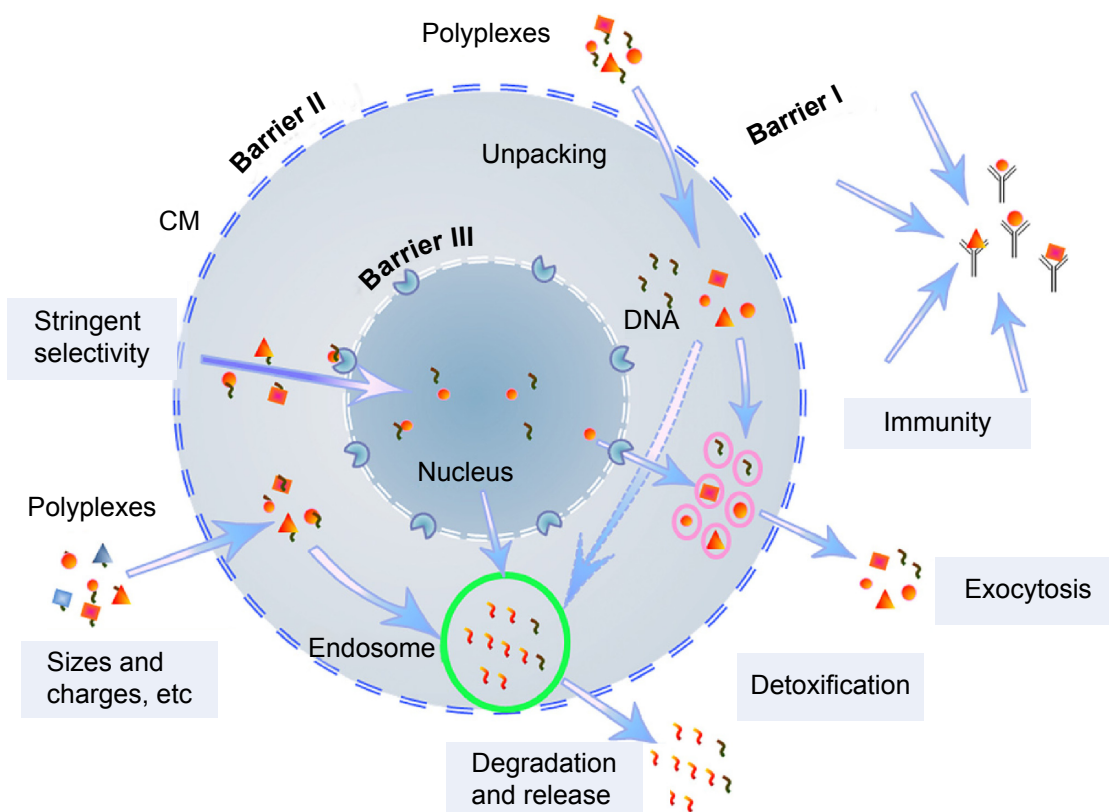


Figure 1 Schematic illustration of self-protection by mammalian cells during cationic polymers-mediated transfection.

Abbreviations: CM, cell membrane; DNA, deoxyribonucleic acid.

for improving transgene expression, which is strictly limited by the cell-nuclear membrane (Figure 1).^{22,23} Just a few of the DNA isolates are able to enter the cell nucleus once the complexes are unpacked within the cell cytoplasm. A successfully studied target ligand was the chlorotoxin (CTX) peptide, which targets the nanovectors to cancer cells.²¹ However, in the case of tumor therapy and analysis of gene functions, a superhigh ratio of transfection is required. In this regard, study and targeting of gene vectors to cell nuclei remains a big challenge.

Recently, cell-nuclear transfer technology has been receiving much attention as a promising strategy to meet the increased requirement for effective transgene expression therapies.¹⁹ Frequently reported elements include proteins/peptides that are able to localize to mammalian cell nuclei, for example, nuclear localization signals (NLS).^{3,24–27} Melittin protein derived from nonviral organisms was used to enhance nuclear access of nonviral gene delivery vectors.²⁸ Novel approaches were developed using polymeric gene carriers conjugated with all-trans-retinoic acid (ATRA).²⁹ Target ligands that are stable, small, and have cell-nuclear localization ability are of interest to researchers.

Myo-inositol (INO) is a biomolecule with crucial functions in eukaryotic cells.^{30–37} The H⁺-Myo-inositol receptors were reported in cancer stem cells (CSC) from various tumors.³⁸ The presence of free myo-inositol has been demonstrated in cell nuclei.³⁹ A series of inositol-related receptors/factors were reported to localize on the nuclear membrane, for example, the inositol 1,4,5-trisphosphate-sensitive Ca²⁺ pool, the InsP receptors, and the nucleocytoplasmic shuttling protein inositol 5-phosphatase SHIP1.^{40,41} Myo-inositol serves as the structural basis for various derivatives, including a number of essential secondary messengers. Myo-inositol and its derivatives, such as phosphatidylglycerol and phosphatidylinositol derivatives, inositol phosphate isoforms, and inositol polyphosphates had metabolism links and are involved in various metabolic pathways in mammalian cells.^{42–46} Among the inositol derivatives, inositol polyphosphates (IP₂–IP₆) play crucial roles in cellular functions including cell growth, endocytosis, migration, differentiation, and apoptosis.^{30,31} IP₃, IP₅, and IP₆ are also involved in gene expression. Inositol(1,4,5)P₃ receptors were revealed at the nuclear envelope of mammalian cells. The PI3K signaling pathway has been widely found in cancer cells, and nuclear transportation of phosphatidylinositol 3-kinase has been observed.^{32,34–37} Importantly, inositol

1,4,5-trisphosphate receptors (IP₃R) have been shown to mediate extracellular adenosine triphosphate (eATP) induced Ca²⁺ transients in cell nuclei rather than in the cytosol.⁴⁷

In our previous study, inositol conjugated PEI800-FA was detected on the cell-nuclear membrane or in cell nuclei with variant levels in the tested cell lines, and transfection efficiency of INO-PEI800 was as high as HMW PEI for some carcinoma cell lines.²² To consolidate INO as a biocompatible ligand for efficient transgene expression, increased ratios of inositols were conjugated to PG6-PEI25k, which is derived from the hyperbranched polyglycerol core and branched HMW PEI25k grafts. As determined, PG6-PEI25k shows enhanced transgene activity and biocompatibility relative to PEI25k but does not enter cell nuclei. The resultant vectors, PG6-PEI-INO with low cytotoxicity, achieved different degrees of enhanced transfection activity as compared with PG6-PEI25k. For PG6-PEI-INO 3 containing a much higher INO ratio at approximately 415 ligands per molecule, transgene expression resulted in >80% of EGFP-positive 293T cells, which demonstrated further enhancement relative to PG6-PEI-INO 1 and 2 that respectively contained 14 and 130 INO ligands per molecule only. Because some cell-nuclear activity, such as the nuclear Ca²⁺ transient, can be specifically induced by eATP,⁴⁷ we then investigated eATP-induced inhibition on EGFP expression, which shows evident differences when comparing the effects of PG6-PEI-INO and PG6-PEI polymers.

Material and methods

Materials

Polyglycerol PG6 ($M_n = 6,170$ g/mol) was obtained from Hyperpolymers GmbH (Freiburg, Germany). Branched PEI25k ($M_w = 25,100$ g/mol), *N*-hydroxysuccinimide (NHS), *N,N'*-dicyclohexylcarbodiimide (DCC), and 1-ethyl-3-(3-dimethylaminopropyl)carbodiimide hydrochloride (EDC) were from Sigma-Aldrich (St Louis, MO, USA). *N*-dimethyl-formamide (DMF) was dried over CaH₂ and distilled under reduced pressure prior to use. 4',6-diamidino-2-phenylindole (DAPI) was purchased from Roche (Branford, CT, USA). 3-(4,5-dimethylthiazol-2-yl)-2,5-diphenyltetrazolium bromide (MTT), trypsin, and penicillin/streptomycin were purchased from Invitrogen

(Carlsbad, CA, USA). All other reagents were purchased from Sinopharm Chemical Reagent Co., Ltd (Shanghai, People's Republic of China). Human embryonic kidney cell line 293T was purchased from the China Center for Typical Culture Collection (Wuhan, People's Republic of China). The cells were cultivated in Dulbecco's Modified Eagle's Medium (DMEM) supplemented with 10% fetal bovine serum, 2 mg/mL NaHCO₃, and 100 units/mL penicillin/streptomycin. Cells were incubated at 37°C in humidified air with 5% CO₂. The reporter plasmid *pEGFP-C1* was obtained from Invitrogen.

Preparing plasmid

Plasmid DNA *pEGFP-C1* was amplified in *Escherichia coli*, extracted with E.Z.N.A. FastFilter Endo-Free Plasmid Maxi Kit (Omega, Norcross, GA, USA). The purified plasmid DNA was stored in TE buffer (supplied with the kit) or deionized (DI) water at a final concentration of 1 mg/mL.

Polymer conjugation

Hyperbranched polymer PG6-PEI25k, which was derived from hyperbranched polyglycerol core ($M_w = 6,170$ g·mol⁻¹, had an average of 90 hydroxyl end-groups per molecule) and branched PEI25k grafts, was synthesized and characterized according to our previous method.¹³ INO (22.5 mg) was added to a 14.3 M NaOH solution (100–200 μL), and the mixture was stirred at room temperature (22°C) for 1 hour. The chloroacetic acid (CAA) (0.3 mg/mL) was added dropwise to the mixture, and the suspension was stirred at 60°C for 12 hours to carboxylate hydroxyls of INO. The solution was then adjusted to acidic (pH 6) with HCl (1 M) to convert –COONa to –COOH. The product was cooled and filtrated to obtain INO-COOH (carboxymethyl INO [CMINO]). The CMINOs were washed with ethanol and distilled under reduced pressure. CMINO was conjugated to PG6-PEI with EDC as the coupling reagent (Table 1). The molar ratios of introduced CMINO to PG6-PEI25k units were approximately 1, 10, and 100 for the three reaction systems. The mixtures were dissolved in DI water, and pH was adjusted to 5–6. The reactions were performed at 42°C for 18 hours, and the reaction mixtures were dialyzed with a dialysis membrane (MWCO: 8,000–12,000 g/mol) against DI

Table 1 Weight ratio of the reactants and molecular weights of PG6-PEI-INO polymers

Polymer	Reactants		M_w (kDa)	Polydispersity (M_w/M_n)
	PG6-PEI25k (mg)	CMINO (mg)		
PG6-PEI-INO 1	2.13	0.0355	455	1.68
PG6-PEI-INO 2	2.13	0.355	465	1.73
PG6-PEI-INO 3	2.13	3.55	542	1.86

Abbreviations: CMINO, carboxymethyl inositol; INO, myo-inositol; PEI, polyethylenimine; PG6, polyglycerol.

water, respectively, and freeze dried under vacuum to obtain PG6-PEI-INO polymers.

FT-IR spectroscopy

Infrared analysis (KBr) of the samples was studied on FT-IR (Fourier transform infrared) spectrometer (Spectrum One; Perkin Elmer, Waltham, MA, USA). Spectra were run in the 4,000–400 cm^{-1} region.

^1H NMR spectroscopy

^1H nuclear magnetic resonance (NMR) spectroscopy was performed on a Varian Inova 600 MHz spectrometer; the solvent was deuterium oxide.

Gel permeation chromatographic ([GPC]/SEC) analysis

The molecular weights of the polymers were determined by combined size-exclusion chromatography and multiangle laser light scattering (SEC–MALLS) analysis. A dual detector system, consisting of a MALLS device (DAWN EOS; Wyatt Technology, Santa Barbara, CA, USA) and an interferometric refractometer (Optilab DSP, Wyatt Technology), was used. PG6-PEI-INO polymers were dissolved in 600 mM of ammonium acetate with a final polymer concentration of 1 mg/mL, and analyzed in ammonium acetate (600 mM) mobile phase. The MALLS detector was operated at a laser wavelength of 690.0 nm. The samples were then determined at a flow rate of 0.3 mL/min.

Agarose gel electrophoresis retardation assays

PG6-PEI-INO polymers were dissolved in 150 mM (or 0.9%) NaCl. PG6-PEI-INO/pDNA (*pEGFP-C1*) complexes were prepared by adding 10 μL of PG6-PEI-INO solutions at serial concentrations to 20 ng of pDNA (20 ng/ μL in 150 mM NaCl). The complexes were incubated at 37°C for 30 minutes, and sampled for electrophoresis on the 0.7% (w/v) agarose gel containing GelRed™ with Tris-acetate-EDTA (TAE) electrophoresis buffer at 80 V. Plasmid DNA bands were visualized on a V-transilluminator with a Vilber Lourmat imaging system (Marne La Vallée, France).

TEM analysis of PG6-PEI-INO/pDNA polyplexes

PG6-PEI-INO/pDNA (*pEGFP-C1*) particles were composited in DI water, and the morphology was determined by transmission electronic microscopy (TEM) on a JEM-100CXII transmission electronic microscope (JEOL, Tokyo, Japan). Aqueous suspensions (3 μL) were placed on

copper grids with Formvar film. The samples were stained by phosphotungstic acid, vacuum-dried and visualized.

Cell viability measurement

Cells were seeded in a 96-well plate at a density of 3×10^3 cells/well in 100 μL of DMEM culture media (10% serum) containing polymers or polymer/*pEGFP-C1* complexes (1.3 μg of *pEGFP-C1* per mL medium) at varied feed ratios. After 52 hours of cultivation, the culture media were replaced with fresh DMEM medium (100 μL) plus 20 μL of MTT (5 mg/mL), and the plate was incubated in the incubator at 37°C for 4 hours. Then the supernatants were replaced with 150 μL of DMSO. After incubation for 15 minutes at 37°C, the absorbance of 50 μL of sample solution was measured in a microplate reader (Bio-Rad 550; Bio-Rad Laboratories Inc., Hercules, CA, USA) at 570 nm. The cell viability was calculated as follows:

$$\text{Cell viability} = \frac{(\text{OD}_{\text{treat}} - \text{OD}_{\text{blank}})}{(\text{OD}_{\text{control}} - \text{OD}_{\text{blank}})} \times 100\%,$$

where OD_{treat} was obtained from the cells treated by materials; $\text{OD}_{\text{control}}$ was obtained from the untreated cells, and OD_{blank} was obtained from the media treated through the same procedure. Each result was obtained from three repeats and expressed as average \pm standard deviation (SD).

In vitro transfection

293T cells were seeded in a 24-well plate at a density of 3×10^4 cells/well in 1 mL of DMEM culture media (10% serum), followed by cultivation for 4 hours. Prior to transfection, 1 μL of *pEGFP-C1* solution (1.3 $\mu\text{g}/\mu\text{L}$ in DI water) was mixed with 1 μL of varied concentrations of PG6-PEI-INO aqueous solutions and diluted with 20 μL of filtrated NaCl (150 mM) solution, followed by vortex and incubation at 37°C for 30 minutes. The complexes were then supplemented to the cell suspension, and coincubated with the cells for 52 hours. The EGFP-positive cell ratio was calculated on a counting chamber with fluorescent phase-contrast microscopy (Olympus IX 70; Olympus Corporation, Tokyo, Japan; at 400 \times), after the cell suspensions were prepared with tryptic digestion to prevent miscounting of the undispersed cells.

Influence of eATP on cell viability and transgene expression

Optimized ratios of PEI25k/*pEGFP-C1* (w/w =1.3), PG6-PEI25k/*pEGFP-C1* (w/w =7), and PG6-PEI-INO 3/*pEGFP-C1* (w/w =7) with fixed dosage of *pEGFP-C1*

(1.3 μg per mL medium) were supplemented with serial concentrations of ATP, respectively, to compare the response of transgene activity of the materials to ATP supplements. The mixtures were incubated at 37°C for 30 minutes before transgene experiments. Detailed MTT assay and transfection procedure were performed in 24-well plates according to the descriptions above. The relative level of transgene expression was calculated as follows:

$$\text{Positive ratio} = \frac{\text{Cell number}_{\text{positive}}}{\text{Cell number}_{\text{total}}} \times 100\%$$

$$\text{Relative expression level} = \frac{\text{Mean positive ratio}_{\text{material}}}{\text{Mean positive ratio}_{\text{control}}} \times 100\%$$

where positive ratio_{material} was obtained from cells treated by materials, and positive ratio_{control} was obtained from cells treated by PEI/*pEGFP-C1*/eATP. Mean positive ratio was achieved by calculating the average value of positive ratios from three repeats.

Fluorescence tracking

The PG6-PEI-INO polymers were labeled with Rhodamine B, which is usually used to stain cytosol instead of cell nuclei. For the three PG6-PEI-INO systems with different INO ratios, identical numbers of amino groups per microgram of polymers were labeled. In brief, PG6-PEI-INO polymers (0.36 mg) and Rhodamine B (2 μg) were dissolved in 5 mL DMF, using NHS and DCC as carboxyl activator and coupling reagent, respectively. The reactions were carried out at 45°C. The mixtures were dialyzed against deionized water at room temperature, and dried in a freeze drier (VirTis, Warminster, PA, USA) to purify PG6-PEI-INO-Rhodamine (Rh)s.

293T cells were seeded in a 6-well plate at a density of 8×10^4 cells/mL media and cultivated for 12 hours. PG6-PEI-INO-Rh (5 $\mu\text{g}/\text{mL}$) was supplemented to the cell cultures and incubated with the cells for 48 hours. The cells were washed with PBS (pH 7.4), stained with DAPI, and washed with PBS. Confocal laser scanning microscopy (CLSM, Leica TCS SP2A OBS; Leica Microsystems, Wetzlar, Germany) was used to record fluorescence within the cells.

Results and discussion

Synthesis and characterization of PG6-PEI-INO polymers

GPC (SEC) analysis showed that PG6-PEI-INO 1, 2, and 3 (Figure 2) had weight average molecular weights (M_w) of 455, 465, and 542 kDa, respectively (Table 1).

FT-IR spectrum showed the peak at 1,724.82 cm^{-1} , depicting $-\text{COOH}$ of CMINO (Figure 3A). The intensity of this peak declined for PG6-PEI-INOs because $-\text{COOH}$ of CMINO reacted with $-\text{NH}_2$ of PEI25k. With the increase in the grafted INO ratio, an increase in the O-H deformation vibration (1,261.96 cm^{-1}) and the fingerprint region of CMINO (799.95 cm^{-1}) was detected in the order of PG6-PEI-INO 1, 2, and 3. The peak (1,462.87 cm^{-1}) indicating the in-plane bending vibration of $-\text{CH}_2$ groups from PG6-PEI and CMINO increased in PG6-PEI-INO 1, 2, and 3. The results indicated successful conjugation of INO to PG6-PEI.

¹H NMR results showed the unreacted $-\text{COOH}$ of CMINO units (10.8 ppm), characteristic PEI proton deviation peaks (2.4–3.0 ppm), and characteristic proton deviation peaks of PG6 and INO (3.0–4.0 ppm) (Figure 3B). With CMINO grafts increased, the ratio of the integral of the 3.0–4.0 ppm peak to that of the 2.0–3.0 ppm peak increased, indicating that an increased number of CMINO molecules were conjugated to PG6-PEI. The molar ratio of PG6 to PEI25k is 1:1, as previously characterized. The ratio of CMINO to PG6-PEI25k units was approximately 1:1, 10:1, and 35:1 in PG6-PEI-INO 1, 2, and 3, respectively. According to the weight average molecular weight (M_w) of PG6-PEI-INOs (Table 1), a PG6-PEI-INO 1 molecule had approximately 14 PEI25k and 14 CMINO units; PG6-PEI-INO 2 had approximately 13 PEI25k and 130 CMINO units; PG6-PEI-INO 3 had approximately 12 PEI25k and 415 CMINO units.

PG6-PEI-INOs composite DNA efficiently

Gel electrophoresis retardation of *pEGFP-C1* demonstrated the DNA-binding activity of PG6-PEI-INOs (Figure 4A). TEM analysis showed that all PG6-PEI-INO polymers could compact plasmid DNA to polyplexes with a diameter of less than 30 nm (Figure 4B). This compacted nanostructure could protect DNA against enzyme degradation and meanwhile benefit cell internalization. With respect to the small particle sizes, it has been reported that the diameter of the nuclear pore complex (NPC) was up to 120 nm and permitted molecules or complexes with diameters of 39 nm to pass through.^{34,48} Therefore, we subsequently determined the transgene expression mediated by PG6-PEI-INO polymers and the cell-nuclear localization of the PG6-PEI-INOs.

Inositol improves biocompatibility of HMW PEI-based vectors

Viability assays showed that both PG6-PEI-INOs/pDNA (w/w = 5–9) (Figure 5A) and an identical weight of PG6-PEI-INOs (Figure 5B) achieved decent biocompatibility

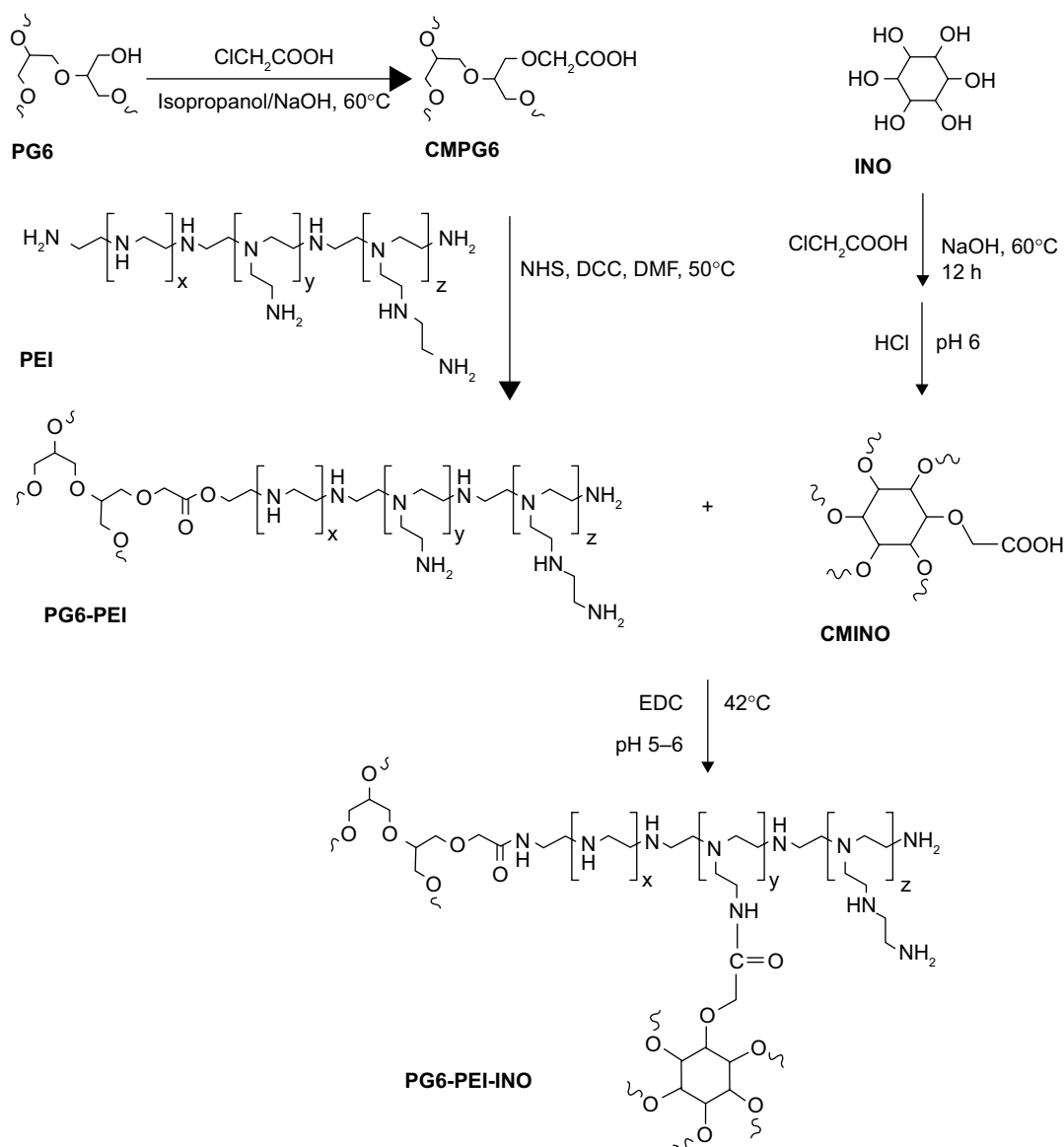


Figure 2 Synthesis route of PG6-PEI-INO polymers.

Abbreviations: CMPG6, carboxymethyl polyglycerol; CMINO, carboxymethyl inositol; DCC, N,N'-dicyclohexylcarbodiimide; DMF, N-dimethyl-formamide; EDC, 1-ethyl-3-(3-dimethylaminopropyl)carbodiimide hydrochloride; INO, myo-inositol; NHS, N-hydroxysuccinimide; PEI, polyethylenimine; PG6, polyglycerol.

(70%–80%) when they were used at high dosage. A previous study indicated that the 293T cell viability was much lower when using an identical dosage of PG6-PEI/*pDNA* or PG6-PEI.¹⁵ Instead, cells treated with an identical dosage of PEI25k/*pEGFP-C1* or unmodified PEI25k had a viability of less than 10% or 8%, respectively. These results demonstrated that INO could further enhance biocompatibility of PG6-PEI25k.

When the weight ratio of PG6-PEI-INO/DNA is 9, the corresponding N/P ratio for PG6-PEI-INO 1, 2, and 3 to DNA has reached 53, 44, and 35, respectively, which is far higher than the permitted dose range of HMW PEI25k/DNA. These results offer an explanation for why PG6-PEI-INO has good biocompatibility. To the question of potential toxicity at the higher doses, for example, whether they produce toxicity

after partial degradation, and how organisms respond, will be addressed by in vivo experiments in future.

Using inositol as efficient ligands for transgene expression

The ability of PG6-PEI-INO to mediate transgene expression was evaluated in 3D 293T cells because they are sensitive indicators. Results showed that the PG6-PEI-INO polymers-mediated EGFP expression effectively without causing cell injury (Figure 6). The expression level was higher with the increase of PG6-PEI-INO. Generally, PG6-PEI-INO 3 containing the highest INO component achieved the highest transgene expression level, as compared with PG6-PEI and PG6-PEI-INO 1 and 2. PG6-PEI-INO

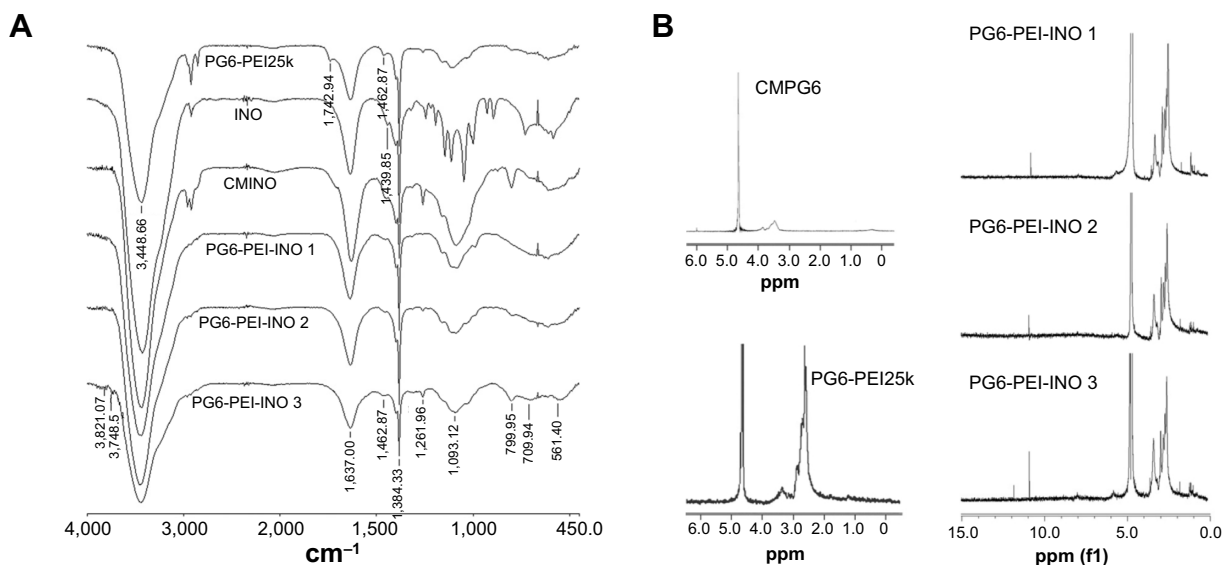


Figure 3 Characterization of the PG6-PEI-INO polymers.

Notes: (A) FT-IR spectra of PG6-PEI-INO 1, PG6-PEI-INO 2, and PG6-PEI-INO 3. (B) ¹H NMR spectra of the polymers. Deuterium oxide was used as the solvent.

Abbreviations: CMINO, carboxymethyl inositol; CMPG6, carboxymethyl polyglycerol; FT-IR, Fourier transform infrared spectroscopy; INO, myo-inositol; NMR, nuclear magnetic resonance; PEI, polyethylenimine; PG6, polyglycerol.

3/*pEGFP-C1* at w/w of 5 and 7 achieved 75% and 82% of positive cells, respectively, which was approximately 19% and 23% higher than that achieved with PG6-PEI/*pEGFP-C1* at identical weight ratios, and was 27% and 34% higher than that achieved by PEI25k/*pEGFP-C1* at the optimal ratio (w/w=1.3 or N/P=10).^{15,49} For PEI25k/*pEGFP-C1* at weight

ratios exceeding 6, cells were severely distorted and/or detached. PG6-PEI-INO 1 with only one INO moiety per molecule showed similar activity as compared with PG6-PEI in general. Compared with PG6-PEI-INO 1/*pEGFP-C1*, PG6-PEI-INO 2/*pEGFP-C1* with more INO grafts achieved more EGFP-positive cells.

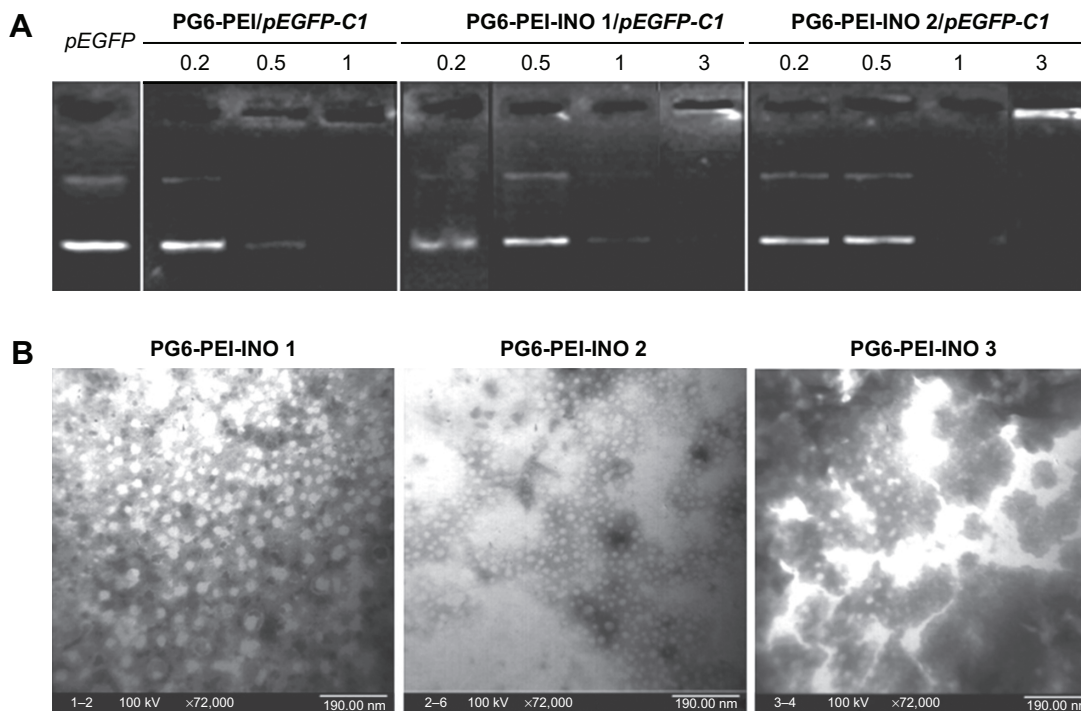


Figure 4 DNA-binding ability of PG6-PEI-INO polymers.

Notes: (A) Agarose gel electrophoresis of PG6-PEI-INO/*pEGFP-C1* complexes at varied weight ratios. (B) Morphologic study of PG6-PEI-INO/*pEGFP-C1* (w/w=5) complexes using transmission electron microscopy.

Abbreviations: INO, myo-inositol; PEI, polyethylenimine; PG6, polyglycerol.

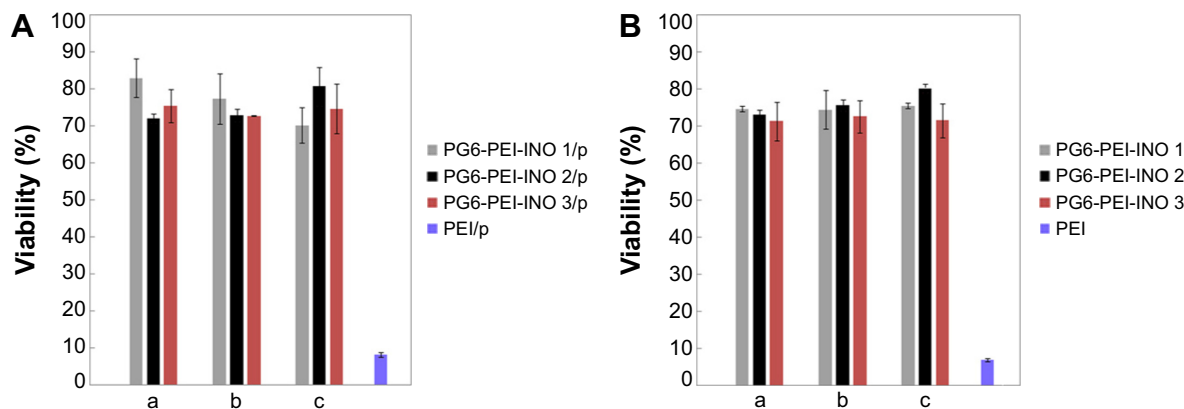


Figure 5 Biocompatibility of the PG6-PEI-INO/plasmid or PG6-PEI-INO polymers.

Notes: (A) MTT analysis of cell viability was performed after 293T cells were cocultivated for 52 hours with PG6-PEI-INOs/plasmid (*pEGFP-C1*), which had weight ratios of 5 (a), 7 (b), and 9 (c), respectively. (B) MTT analysis of cell viability was performed after 293T cells were cocultivated with identical dosages of PG6-PEI-INOs for 52 hours. Cells were treated with PEI25k/*pEGFP-C1* at a weight ratio of 6, or with an identical dosage of PEI25k as the control. DNA was used at 1.3 μg of *pEGFP-C1* per mL medium. **Abbreviations:** INO, myo-inositol; PEI, polyethylenimine; PG6, polyglycerol; p, plasmid (*pEGFP-C1*).

When the weight ratios to DNA were 1 and 3, the transfection activity increased in the order of PG6-PEI < PG6-PEI-INO 1 < PG6-PEI-INO 2. When the weight ratios were 5 and 7, no apparent increase was observed among the three systems. Compared with PG6-PEI-INO 3, which had approximately 12 PEI25k and 415 CMINO units and showed the highest transfection activity, a PG6-PEI-INO 1 molecule had approximately 14 PG6, 14 PEI25k, and only 14 CMINO units, and PG6-PEI-INO 2 had approximately 13 PG6, 13 PEI25k, and 130 CMINO units. Conjugation with INO will reduce $-\text{NH}_2$ termini of PEI25k and therefore lower the DNA-binding ability of PEI25k. On the other hand, conjugation with INO increases biocompatibility of PEI25k and accumulation of PG6-PEI-INOs in cell nuclei, as will be illustrated in the subsequent experiment. Therefore, we deem that a balance exists between

the two aspects. When the number of INO is high enough to achieve a high accumulation of gene vectors in cell nuclei and meet the requirement for DNA binding/protection simultaneously, then transgene expression levels tended to increase as a result of transcription from DNA within cell nuclei and the subsequent translation from mRNA in cytoplasm. From these results, we observed that as the proportion of the INO increased, the efficiency of identical dosages of PG6-PEI-INOs to composite DNA was similar (Figure 4), indicating that DNA-binding ability might be primarily related to polymer structure. PG6-PEI-INO 3 at identical dosages with the lowest N/P ratios showed the highest transgene expression efficiency at most tested weight ratios to DNA, without obvious impairment in cell viability, demonstrating the potentiality of using inositol as an efficient ligand for transgene expression.

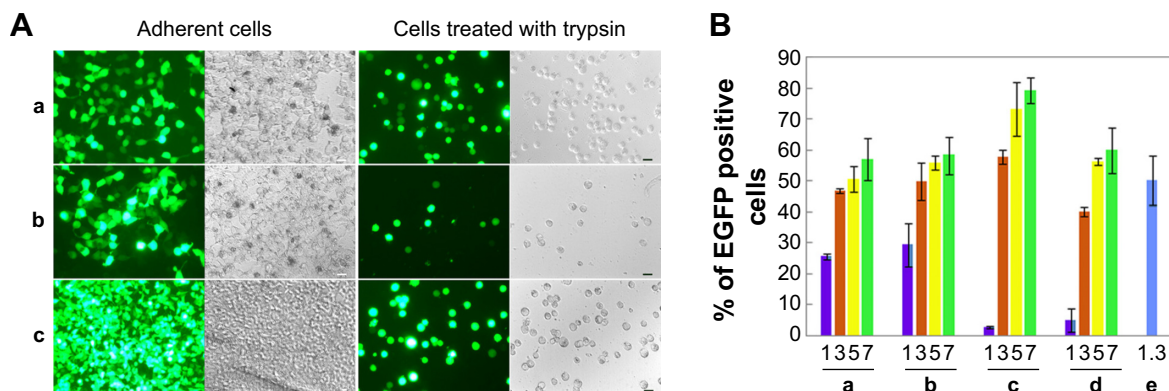


Figure 6 Transfection activities of PG6-PEI-INO polymers.

Notes: (A) Transgene expression reported by protein EGFP in 293T cell line treated with (a) PG6-PEI-INO 1/*pEGFP-C1*, (b) PG6-PEI-INO 2/*pEGFP-C1*, and (c) PG6-PEI-INO 3/*pEGFP-C1* complexes at weight ratio of 7, respectively. Plasmid *pEGFP-C1* was used at 1.3 μg per mL culture medium. The cells were cultivated for 52 hours. The adherent cells and the cell suspensions achieved with trypsin treatment were analyzed by phase-contrast fluorescent microscopy. Scale bar: 15 μm . (B) EGFP-positive cell ratios achieved by transgene expression mediated by PG6-PEI-INO polymers. The 293T cells were transfected using the following agents: (a) PG6-PEI-INO 1, (b) PG6-PEI-INO 2, (c) PG6-PEI-INO 3, (d) PG6-PEI at varied weight ratios to *pEGFP-C1*, and (e) the PEI25k control at its optimal weight ratio (1.3) to *pEGFP-C1* (1.3 μg of *pEGFP-C1* per mL cell culture). **Abbreviations:** INO, myo-inositol; PEI, polyethylenimine; PG6, polyglycerol; EGFP, enhanced green fluorescent protein.

In our previous studies, INO-PEI800-FA was constructed and demonstrated efficient transgene activity. However, on the basis of low molecular weight PEI without any transgene activity, the transfection should still be limited. Partially attributed to the greatly enhanced biocompatibility compared with PEI25k, PG6-PEI-INO developed in this study can be used at high dosages without apparent injury to 293T cells, and this may allow the consequent generation of much higher transgene expression levels in the 293T cell line. It has been revealed that PEI800-INO performs better in carcinoma cells than in 293T. The performance of PG6-PEI-INO in carcinoma cells is the goal of our next study.

It is noteworthy that, along with the increase in myo-inositol from 1 to 35 per PEI25k unit within polymeric molecule, PG6-PEI-INO polymers showed a corresponding increase in the transgenic efficiency. As compared with the current commercial reagent Lipofectamine (20%–60% transfection rate depending on cell types),^{50,51} PG6-PEI-INO polymers based on HMW PEI can obtain a higher transgene expression rate in the presence of serum and antibiotics. For 293T cell lines, this high transfection rate (>80%) achieved with PG6-PEI-INO 3 is higher than commercial Lipofectamine, and the efficiency can be realized in a considerably higher and wider range of dosages with reasonable viability. Lipofectamine can achieve higher efficiency when used for transient RNA delivery. This is because the RNA does not need to pass through the nuclear membrane. Whether the myo-inositol group can improve the transfection activity of vectors like Lipofectamine 3000, Fugene 6, and chitosan-based vectors is a topic worthy of study, and this work is currently ongoing in our laboratory.

Extracellular ATP increases viability of cells treated with PG6-PEI-INOs/pDNA

Since eATP can influence cell-nuclear activity and transport (including transmembrane or transnuclear transport) and because the metabolism of inositol and its derivatives are related to ATP in some essential aspects,^{31,47,52–54} we investigated the influence of eATP on cell viability and transgene expression with PG6-PEI-INO 3 containing the highest contents of INO as a representative medium for transfection. PEI25k and PG6-PEI without nuclear entrance ability were set as negative controls.

Results indicated that eATP clearly stimulated propagation of 293T cells transfected with PG6-PEI-INO 3/pEGFP-C1, compared with those transfected with PEI25k/pEGFP-C1 or PG6-PEI/pEGFP-C1 (Figure 7). PG6-PEI/pEGFP-C1 transfected cells doubled in growth at 3.3 µg/mL of

eATP, and then decreased with further increases in eATP. The viability of PEI25k/pEGFP-C1 treated cells was not significantly affected by eATP. Therefore, with respect to cell viability, response levels to eATP differed because of the biocompatible PG6 and INO moieties. Since polyglycerol and inositol can be metabolized more efficiently when ATP is increased, this may increase the cell viability. In addition, derivatives of the INO ligands may also participate in PI3K signaling pathways that are required by ATP-stimulated cell proliferation.⁵⁵

Extracellular ATP inhibited transgene activity of PG6-PEI-INO

The influence of eATP on transfection with PG6-PEI-INO 3/pEGFP-C1, PG6-PEI/pEGFP-C1, and PEI25k/pEGFP-C1 at optimized weight ratios was analyzed. With the supplementation of eATP, cells transfected with the PG6-PEI-INO 3/pEGFP-C1 reagent declined to <1%. Transfection with PEI25k/pEGFP-C1 was not apparently influenced by eATP (Figure 8). Compared with PG6-PEI-INO, the influence of eATP on PG6-PEI was much smaller. Since eATP did not reduce the transfection activity of PEI25k or PG6-PEI apparently, we deduced that the transgene activity of PG6-PEI-INO 3 should be related to certain intracellular pathways, rather than weakening of DNA-binding activity.

Distribution of PG6-PEI-INO in cell nuclei

By 48 hours of incubation, all the INO conjugated vectors were internalized by 293T cells at high frequencies. Results

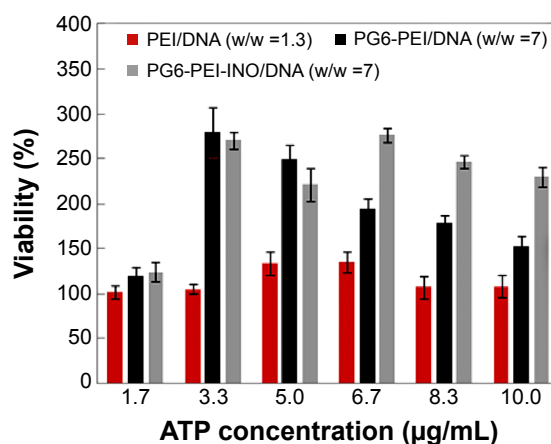


Figure 7 Effect of extracellular ATP on the growth rate of 293T cells transfected with various polymer/complexes (at optimal weight ratio for transfection).

Notes: MTT analyses of cell viability were performed after the 293T cells were cocultivated with the materials for 44 hours. About 1.3 µg of plasmid pEGFP-C1 was used per microliter of cell culture.

Abbreviations: ATP, adenosine triphosphate; INO, myo-inositol; PEI, polyethylenimine; PG6, polyglycerol.

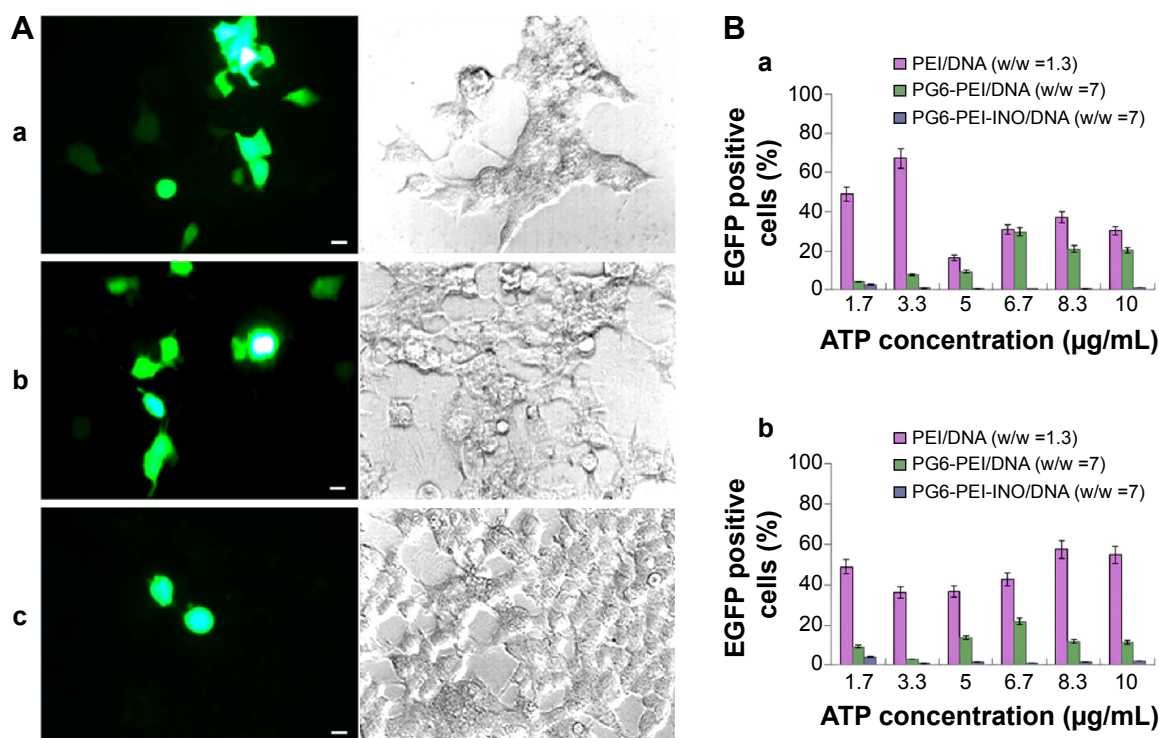


Figure 8 Inhibition of extracellular ATP on transgene activity of PG6-PEI-INO.

Notes: (A) The 293T cells were treated with (a) PEI25k/pEGFP-C1 (w/w = 1.3), (b) PG6-PEI/pEGFP-C1 (w/w = 7), and (c) PG6-PEI-INO 3/pEGFP-C1 (w/w = 7) for 96 hours, respectively. Extracellular ATP was used at 1.7 µg per mL culture medium. Scale bar: 10 µm. (B) EGFP-positive 293T cell ratios mediated by polymers/DNA/ATP. Plasmid DNA (pEGFP-C1) was used at 1.3 µg per mL culture medium. The cells were treated with the polymers/DNA/ATP for 44 hours (a) and 96 hours (b), respectively.

Abbreviations: ATP, adenosine triphosphate; INO, myo-inositol; PEI, polyethylenimine; PG6, polyglycerol.

of the MTT analysis indicated high viability of the cells. Compared with PG6-PEI-INO-Rh 1 with approximately one INO moiety grafted per PEI unit, PG6-PEI-INO-Rh 2 and 3 with increased number of INO grafts had increased accumulation within the cell nuclei (Figure 9). More than 80% of the 293T cells showed distinct nuclear access of the PG6-PEI-INO-Rh 3 polymers. Of note, PG6-PEI-INO-Rh 3 polymers were concentrated to cell nuclei from the cytoplasm. We believe that this difference between PG6-PEI-INO-Rh 1, 2, and 3 should be related to the mechanisms relevant to the transport of nanoparticles mediated by the NPC. As reported, this NPC-mediated transport of various large molecules (such as DNAs, RNAs) is related to the Ca^{2+} pump.⁵⁶ In some mammalian cell nuclei, extracellular ATP activates purinergic receptors such as P2Y2 and P2X4, which induces an increase in the free Ca^{2+} concentration in the cell nuclei. To balance the Ca^{2+} transient, cADP-ribose and the intracellular messenger, inositol 1,4,5-triphosphate [$Ins(1,4,5)P_3$, IP_3], can trigger the release of partial nuclear Ca^{2+} through the actions of inositol 1,4,5-triphosphate receptors (IP_3R), indicating a role for extracellular ATP in regulating nuclear function, by increasing nuclear

Ca^{2+} concentrations.^{47,56–60} Since inositol is metabolically linked to IP_3 within mammalian cells,^{42–46} this course may consume INO ligands in the PG6-PEI-INO vectors and result in unpacking of vector/pDNA complexes, and further inhibit transgene expression. Relevant mechanisms were predicted and shown in Figure 10. This was further demonstrated by the less negative influence of eATP on PEI25k or PG6-PEI-mediated EGFP expression (Figure 8). Although cells treated with PG6-PEI/pEGFP-C1 were inhibited by eATP more apparently than PEI25k/pEGFP-C1-treated cells, their variance is considerably smaller compared with cells treated with PG6-PEI-INO 3/pEGFP-C1, which approaches complete inhibition.

It is known that PEIs can help nucleotides escape from endosomal degradation through the “proton-sponge effect”.^{6,12} However, the ability of PEIs to mediate transgene expression was limited. LMW PEIs lack transfection activity, whereas mid-to-high concentration of HMW PEIs can damage cell membranes.⁶¹ In general, current gene vectors lack the ability to locate in cell nuclei, and it was deemed that nuclear import of therapeutic DNA or RNA occurred after they were released from the PEI transgene systems.^{62–64}

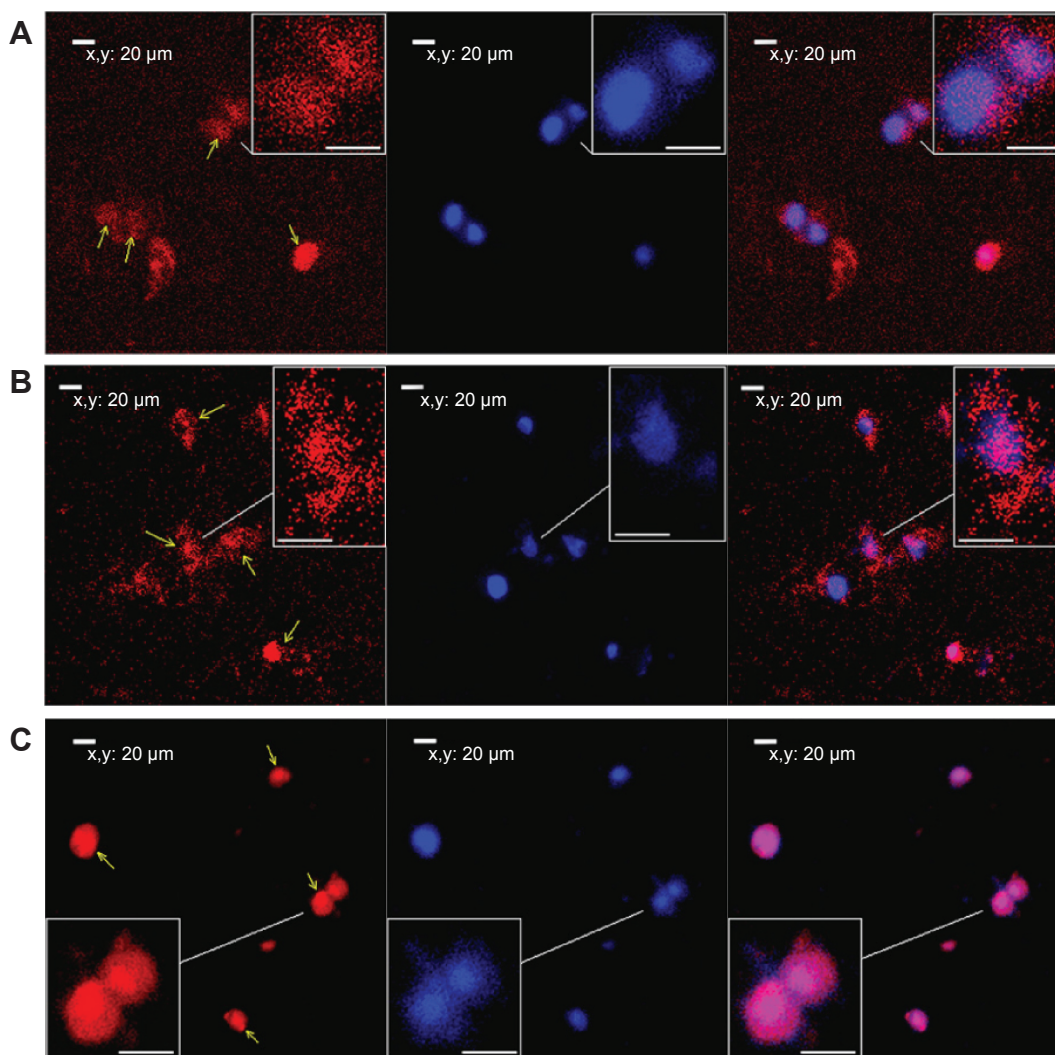


Figure 9 Fluorescence tracking of PG6-PEI-INO polymers in 293T cell nuclei.

Notes: Fluorescence was analyzed after the 293T cells were cocultivated for 48 hours with (A) PG6-PEI-INO-Rh 1, (B) PG6-PEI-INO-Rh 2, and (C) PG6-PEI-INO-Rh 3, which had increased inositol ligands per molecule (1:1, 1:10, and 1:35, respectively). Accumulation of PG6-PEI-INO-Rhs in cell nuclei was indicated with arrows. Scale bar in magnified images: 15 μ m. Red fluorescence shows Rhodamine B (Emission: \sim 572 nm). Blue fluorescence shows the cell nuclei stained with DAPI (Emission: \sim 461 nm when bound with DNA). Merged images in purple color show the PG6-PEI-INO-Rh polymers in cell nuclei.

Abbreviations: DAPI, (4',6-diamidino-2-phenylindole); INO, myo-inositol; PEI, polyethylenimine; PG6, polyglycerol; Rh, Rhodamine.

As commonly accepted, the barrier of nuclear membrane can largely limit transgene expression. Therefore, researchers are currently interested in investigating cationic gene vectors that can locate in cell nuclei.^{29,63,64} Using PG6-PEI25k as the platform, the ability of the PG6-PEI-INO polymers to enter cell nuclei and to mediate efficient transgene expression was found to increase with their INO moiety numbers, as reported by fluorescent tracking and EGFP expression. Therefore, the INO might be a potential ligand for efficient transgene expression.

As compared with PEI800-INO-FA, the higher frequency exhibited by PG6-PEI25k-INO of entering cell nuclei of

293T should be related to the enhanced water solubility and improvement in cell internalization.²²

Conclusion

HMW PEI has high transfection activity, but its cytotoxicity and inability to pass through the nuclear barrier are deemed as shortcomings. In our previous studies based on LMW PEI without transfection activity but possessing good cell compatibility, myo-inositol was introduced. The resultant polymers (PEI-INO) have obvious transfection activity, and in some experimental cell lines, they exhibit transfection activity near HMW PEI. In order to explore myo-inositol as

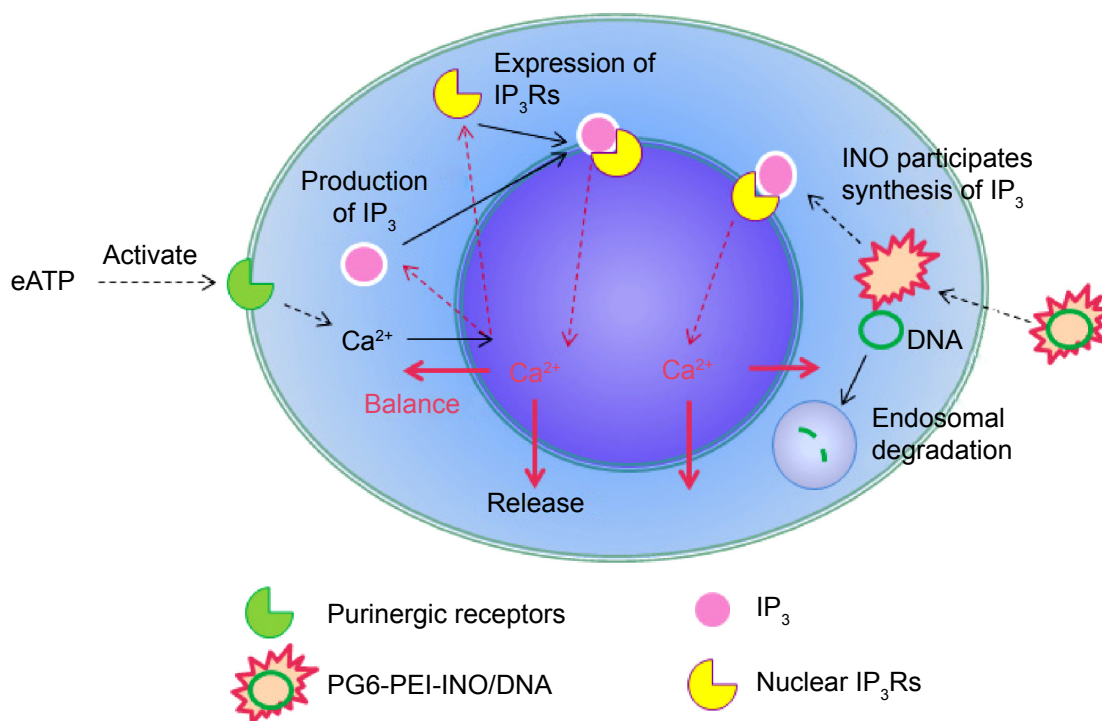


Figure 10 Prediction of eATP function during the delivery of plasmid DNA with PG6-PEI-INO as mediator.

Abbreviations: eATP, extracellular adenosine triphosphate; INO, myo-inositol; IP, inositol polyphosphate; IP₃R, inositol 1,4,5-trisphosphate receptor; PEI, polyethylenimine; PG6, polyglycerol.

a potential ligand for enhancing transfection efficiency and improving cell compatibility, and to further expand the range of applications for HMW PEI, we studied PG6-PEI. PG6-PEI was synthesized by grafting HMW PEI to the functional hydroxyl termini of the branched biocompatible polyglycerol, as a platform in this report. Previous research showed that LMW PEI conjugated with inositol can partially enter cell nuclei, and, therefore, the properties of myo-inositol with nuclear localization capability are a major topic of attention for our group.

Since INO is a natural biomolecule that impacts many important physiological activities, it was introduced as a potential biological moiety to PG6-PEI in this study through covalent reaction. The resultant polymers, PG6-PEI-INO macromolecules, were characterized by FT-IR spectrometry, ¹H NMR spectroscopy, and combined SEC-MALLS analysis. Gel electrophoresis retardation and TEM analysis demonstrated the DNA-binding activity of PG6-PEI-INOs, and all the polymers could compact plasmid DNA and generate nanoparticles with diameters of less than 30 nm. Enhancement of effective transgene reported by EGFP expression was achieved in an actively propagating 3D 293T cell line using PG6-PEI-INO systems as mediators. Meanwhile, PG6-PEI-INO polymers presented reduced cytotoxicity when compared with PG6-PEI and PEI25k polymers. In the presence

of eATP, the transgene expression level was inhibited, while cell growth was stimulated. CLSM analysis demonstrated the ability of PG6-PEI-INO polymers to enter the cell nuclei of 3D 293T cells. With an increase in conjugated INO, both the level of transgene activity and the accumulation of the PG6-PEI-INO polymers in the cell nuclei were elevated.

In conclusion, this work showed the potentiality of INO to be used as a ligand for efficient transgene expression applied in a wide area including transgene therapy and phenotypic analysis of a cell population.

Acknowledgments

We thank the National Nature Science Foundation of China (31300650 and 31270790), the Key Project of Fujian Province (2013N0039, 2012Y0070), the Nature Science Foundation of Fujian Province (2013J01151), the Science Foundation for Post Doctorate Research of Wuhan University of China (203-180462), the National Thousand Talents Program of China, and the Scientific Research Starting Foundation for Returned Overseas Chinese Scholars of State Human Resource Ministry of China for support on this work.

Disclosure

The authors report no conflicts of interest in this work.

References

1. Verma IM, Somia N. Gene therapy – promises, problems and prospects. *Nature*. 1997;389(6648):239–242.
2. Pack DW, Hoffman AS, Pun S, Stayton PS. Design and development of polymers for gene delivery. *Nat Rev Drug Discov*. 2005;4(7):581–593.
3. Carlisle RC, Bettinger T, Ogris M, Hale S, Mautner V, Seymour LW. Adenovirus hexon protein enhances nuclear delivery and increases transgene expression of polyethylenimine/plasmid DNA vectors. *Mol Ther*. 2001;4(5):473–483.
4. Kay MA. AAV vectors and tumorigenicity. *Nat Biotechnol*. 2007;25(10):1111–1113.
5. Ferber D. Gene therapy: safer and virus-free? *Science*. 2001;294(5547):1638–1642.
6. Boussif O, Lezoualch F, Zanta MA, et al. A versatile vector for gene and oligonucleotide transfer into cells in culture and in-vivo – polyethylenimine. *Proc Natl Acad Sci U S A*. 1995;92(16):7297–7301.
7. Putnam D. Polymers for gene delivery across length scales. *Nat Mater*. 2006;5(6):439–451.
8. Ohlfest JR, Freese AB, Largaespa DA. Nonviral vectors for cancer gene therapy: prospects for integrating vectors and combination therapies. *Curr Gene Ther*. 2005;5(6):629–641.
9. Glover DJ, Lipps HJ, Jans DA. Towards safe, non-viral therapeutic gene expression in humans. *Nat Rev Genet*. 2005;6(4):299–310.
10. Ogris M, Wagner E. Targeting tumors with non-viral gene delivery systems. *Drug Discov Today*. 2002;7(8):479–485.
11. Wagner E. Targeting tumors with non-viral gene delivery systems. *J Gene Med*. 2003;5(3):S7–S8.
12. Godbey WT, Wu KK, Mikos AG. Poly(ethylenimine) and its role in gene delivery. *J Control Release*. 1999;60(2–3):149–160.
13. Hu CH, Zhang L, Wu DQ, Cheng SX, Zhang XZ, Zhuo RX. Heparin-modified PEI encapsulated in thermosensitive hydrogels for efficient gene delivery and expression. *J Mater Chem*. 2009;19(20):3189–3197.
14. Kreppel F, Kochanek S. Modification of adenovirus gene transfer vectors with synthetic polymers: a scientific review and technical guide. *Mol Ther*. 2008;16(1):16–29.
15. Zhang L, Hu CH, Cheng SX, Zhuo RX. PEI grafted hyperbranched polymers with polyglycerol as a core for gene delivery. *Colloids Surf B Biointerfaces*. 2010;76(2):427–433.
16. Neu M, Germershaus O, Behe M, Kissel T. Bioreversibly cross-linked polyplexes of PEI and high molecular weight PEG show extended circulation times in vivo. *J Control Release*. 2007;124(1–2):69–80.
17. Bivas-Benita M, Romeijn S, Junginger HE, Borchard G. PLGA-PEI nanoparticles for gene delivery to pulmonary epithelium. *Eur J Pharm Biopharm*. 2004;58(1):1–6.
18. Chiu SH, Ueno NT, Lee RJ. Tumor-targeted gene delivery via anti-HER2 antibody (trastuzumab, Herceptin®) conjugated polyethylenimine. *J Control Release*. 2004;97(2):357–369.
19. Kunath K, Merdan T, Hegener O, Haberland H, Kissel T. Integrin targeting using RGD-PEI conjugates for in vitro gene transfer. *J Gene Med*. 2003;5(7):588–599.
20. Zanta MA, Boussif O, Adib A, Behr JP. In vitro gene delivery to hepatocytes with galactosylated polyethylenimine. *Bioconjugate Chem*. 1997;8(6):839–844.
21. Veisesh O, Kievit FM, Gunn JW, Ratner BD, Zhang MQ. A ligand-mediated nanovector for targeted gene delivery and transfection in cancer cells. *Biomaterials*. 2009;30(4):649–657.
22. Zhang L, Fan Y, Wu Y. Inositol based non-viral vectors for transgene expression in human cervical carcinoma and hepatoma cell lines. *Biomaterials*. 2014;35(6):2039–2050.
23. Zhang C, Gao SJ, Jiang W, et al. Targeted minicircle DNA delivery using folate-poly(ethylene glycol)-polyethylenimine as non-viral carrier. *Biomaterials*. 2010;31(23):6075–6086.
24. Zanta MA, Belguise-Valladier P, Behr JP. Gene delivery: a single nuclear localization signal peptide is sufficient to carry DNA to the cell nucleus. *Proc Natl Acad Sci U S A*. 1999;96(1):91–96.
25. Manickam DS, Oupicky D. Multiblock reducible copolypeptides containing histidine-rich and nuclear localization sequences for gene delivery. *Bioconjugate Chem*. 2006;17(6):1395–1403.
26. Jeon O, Lim HW, Lee M, Song SJ, Kim BS. Poly(L-lactide-co-glycolide) nanospheres conjugated with a nuclear localization signal for delivery of plasmid DNA. *J Drug Target*. 2007;15(3):190–198.
27. Yoo HS, Jeong SY. Nuclear targeting of non-viral gene carriers using psoralen-nuclear localization signal (NLS) conjugates. *Eur J Pharm Biopharm*. 2007;66(1):28–33.
28. Ogris M, Carlisle RC, Bettinger T, Seymour LW. Melittin enables efficient vesicular escape and enhanced nuclear access of nonviral gene delivery vectors. *J Biol Chem*. 2001;276(50):47550–47555.
29. Park KM, Kang HC, Cho JK, et al. All-trans-retinoic acid (ATRA)-grafted polymeric gene carriers for nuclear translocation and cell growth control. *Biomaterials*. 2009;30(13):2642–2652.
30. Huang HM, Toral-Barza L, Thaler H, Tofel-Grehl B, Gibson GE. Inositol phosphates and intracellular calcium after bradykinin stimulation in fibroblasts from young, normal aged and Alzheimer donors. *Neurobiol Aging*. 1991;12(5):469–473.
31. Shen XT, Xiao H, Ranallo R, Wu WH, Wu C. Modulation of ATP-dependent chromatin-remodeling complexes by inositol polyphosphates. *Science*. 2003;299(5603):112–114.
32. Steger DJ, Haswell ES, Miller AL, Wente SR, O’Shea EK. Regulation of chromatin remodeling by inositol polyphosphates. *Science*. 2003;299(5603):114–116.
33. Jia SD, Roberts TM, Zhao JJ. Should individual PI3 kinase isoforms be targeted in cancer? *Curr Opin Cell Biol*. 2009;21(2):199–208.
34. Batrakou DG, Kerr ARW, Schirmer EC. Comparative proteomic analyses of the nuclear envelope and pore complex suggests a wide range of heretofore unexpected functions. *J Proteomics*. 2009;72(1):56–70.
35. Missirolis S, Etro D, Buontempo F, Ye KQ, Capitani S, Neri LM. Nuclear translocation of active AKT is required for erythroid differentiation in erythropoietin treated K562 erythroleukemia cells. *Int J Biochem Cell Biol*. 2009;41(3):570–577.
36. Humbert JP, Matter N, Artault JC, Koppler P, Malviya AN. Inositol 1,4,5-trisphosphate receptor is located to the inner nuclear membrane vindicating regulation of nuclear calcium signaling by inositol 1,4,5-trisphosphate – discrete distribution of inositol phosphate receptors to inner and outer nuclear membranes. *J Biol Chem*. 1996;271(1):478–485.
37. Lanini L, Bachs O, Carafoli E. The calcium-pump of the liver nuclear-membrane is identical to that of endoplasmic-reticulum. *J Biol Chem*. 1992;267(16):11548–11552.
38. Lee DG, Lee JH, Choi BK, et al. H⁺-myo-inositol transporter SLC2A13 as a potential marker for cancer stem cells in an oral squamous cell carcinoma. *Curr Cancer Drug Targets*. 2011;11(8):966–975.
39. Narumi K, Tsumita T. Isolation and identification of free myo-inositol and scyllo-inositol in cell nuclei. *Jpn J Exp Med*. 1969;39(4):409–415.
40. Mishra OP, Qayyum I, Delivoria-Papadopoulos M. Hypoxia-induced modification of the inositol triphosphate receptor in neuronal nuclei of newborn piglets: role of nitric oxide. *J Neurosci Res*. 2003;74(2):333–338.
41. Nalaskowski MM, Metzner A, Brehm MA, et al. The inositol 5-phosphatase SHIP1 is a nucleo-cytoplasmic shuttling protein and enzymatically active in cell nuclei. *Cell Signal*. 2012;24(3):621–628.
42. Carrasco D, Allende CC, Allende JE. The incorporation of myo-inositol into phosphatidylinositol derivatives is stimulated during hormone-induced meiotic maturation of amphibian oocytes. *Exp Cell Res*. 1990;191(2):313–318.
43. Voglmayr JK. Alpha-chlorohydrin-induced changes in the distribution of free myo-inositol and prostaglandin F2alpha, and synthesis of phosphatidylinositol in the rat epididymis. *Biol Reprod*. 1974;11(5):593–600.
44. Chu SW, Geyer RP. myo-Inositol action on gerbil intestine. Association of phosphatidylinositol metabolism with lipid clearance. *Biochim Biophys Acta*. 1982;710(1):63–70.
45. Abel K, Anderson RA, Shears SB. Phosphatidylinositol and inositol phosphate metabolism. *J Cell Sci*. 2001;114(Pt 12):2207–2208.

46. Mattingly RR, Stephens LR, Irvine RF, Garrison JC. Effects of transformation with the v-src oncogene on inositol phosphate metabolism in rat-1 fibroblasts. D-myo-inositol 1,4,5,6-tetrakisphosphate is increased in v-src-transformed rat-1 fibroblasts and can be synthesized from D-myo-inositol 1,3,4-trisphosphate in cytosolic extracts. *J Biol Chem.* 1991;266(23):15144–15153.
47. Chen Z, Li ZZ, Peng G, et al. Extracellular ATP-induced nuclear Ca²⁺ transient is mediated by inositol 1,4,5-trisphosphate receptors in mouse pancreatic beta-cells. *Biochem Biophys Res Commun.* 2009;382(2):381–384.
48. Pante N, Kann M. Nuclear pore complex is able to transport macromolecules with diameters of about 39 nm. *Mol Biol Cell.* 2002;13(2):425–434.
49. Honore I, Grosse S, Frison N, Favatier F, Monsigny M, Fajac I. Transcription of plasmid DNA: influence of plasmid DNA/polyethylenimine complex formation. *J Control Release.* 2005;107(3):537–546.
50. Liu CX, Chen ZJ, Yu WY, Zhang N. Novel cationic 6-lauroxyhexyl lysinate modified poly(lactic acid)-poly(ethylene glycol) nanoparticles enhance gene transfection. *J Colloid Interf Sci.* 2011;354(2):528–535.
51. Tripathi SK, Goyal R, Kumar P, Gupta KC. Linear polyethylenimine-graft-chitosan copolymers as efficient DNA/siRNA delivery vectors in vitro and in vivo. *Nanomedicine.* 2012;8(3):337–345.
52. Arkhammar P, Hallberg A, Kindmark H, Nilsson T, Rorsman P, Berggren PO. Extracellular ATP increases cytoplasmic free Ca²⁺ concentration in clonal insulin-producing Rinn5f cells – a mechanism involving direct interaction with both release and refilling of the inositol 1,4,5-trisphosphate-sensitive Ca²⁺ pool. *Biochem J.* 1990;265(1):203–211.
53. Nagy R, Grob H, Weder B, et al. The Arabidopsis ATP-binding cassette protein AtMRP5/AtABCC5 is a high affinity inositol hexakisphosphate transporter involved in guard cell signaling and phytate storage. *J Biol Chem.* 2009;284(48):33614–33622.
54. Gerasimenko OV, Gerasimenko JV, Tepikin AV, Petersen OH. ATP-dependent accumulation and inositol trisphosphate-mediated or cyclic ADP-ribose-mediated release of Ca²⁺ from the nuclear-envelope. *Cell.* 1995;80(3):439–444.
55. Wilden PA, Agazie YM, Kaufman R, Halenda SP. ATP-stimulated smooth muscle cell proliferation requires independent ERK and PI3K signaling pathways. *Am J Physiol.* 1998;275(4 Pt 2):H1209–H1215.
56. Paulillo SM, Powers MA, Ullman KS, Fahrenkrog B. Changes in nucleoporin domain topology in response to chemical effectors. *J Mol Biol.* 2006;363(1):39–50.
57. Bustamante JO, Michelette ER, Geibel JP, Dean DA, Hanover JA, McDonnell TJ. Calcium, ATP and nuclear pore channel gating. *Pflugers Arch.* 2000;439(4):433–444.
58. Nicotera P, Orrenius S, Nilsson T, Berggren PO. An inositol 1,4,5-trisphosphate-sensitive Ca²⁺ pool in liver nuclei. *Proc Natl Acad Sci U S A.* 1990;87(17):6858–6862.
59. Elsing C, Georgiev T, Hubner CA, Boger R, Stremmel W, Schlenker T. Extracellular ATP induces cytoplasmic and nuclear Ca²⁺ transients via P2Y₂ receptor in human biliary epithelial cancer cells (Mz-Cha-1). *Anticancer Res.* 2012;32(9):3759–3767.
60. Guihard G, Proteau S, Rousseau E. Does the nuclear envelope contain two types of ligand-gated Ca²⁺ release channels? *FEBS Lett.* 1997;414(1):89–94.
61. Kunath K, von Harpe A, Fischer D, et al. Low-molecular-weight polyethylenimine as a non-viral vector for DNA delivery: comparison of physicochemical properties, transfection efficiency and in vivo distribution with high-molecular-weight polyethylenimine. *J Control Release.* 2003;89(1):113–125.
62. Kanazawa T, Takashima Y, Murakoshi M, Nakai Y, Okada H. Enhancement of gene transfection into human dendritic cells using cationic PLGA nanospheres with a synthesized nuclear localization signal. *Int J Pharm.* 2009;379(1):187–195.
63. Hebert E. Improvement of exogenous DNA nuclear importation by nuclear localization signal-bearing vectors: a promising way for non-viral gene therapy? *Biol Cell.* 2003;95(2):59–68.
64. Ledley FD. Pharmaceutical approach to somatic gene therapy. *Pharm Res.* 1996;13(11):1595–1614.

International Journal of Nanomedicine

Publish your work in this journal

The International Journal of Nanomedicine is an international, peer-reviewed journal focusing on the application of nanotechnology in diagnostics, therapeutics, and drug delivery systems throughout the biomedical field. This journal is indexed on PubMed Central, MedLine, CAS, SciSearch®, Current Contents®/Clinical Medicine,

Submit your manuscript here: <http://www.dovepress.com/international-journal-of-nanomedicine-journal>

Dovepress

Journal Citation Reports/Science Edition, EMBase, Scopus and the Elsevier Bibliographic databases. The manuscript management system is completely online and includes a very quick and fair peer-review system, which is all easy to use. Visit <http://www.dovepress.com/testimonials.php> to read real quotes from published authors.